NASA TECHNICAL MEMORANDUM

NASA TM X-73509

NASA TM X-73509

A 30-CM DIAMETER ARGON ION SOURCE

by J. S. Sovey
Lewis Research Center
Cleveland, Ohio 44135

TECHNICAL PAPER to be presented at the
Twelfth International Electric Propulsion Conference sponsored by the
American Institute of Aeronautics and Astronautics
Key Biscayne, Florida, November 15-17, 1976

A 30-cm DIAMETER ARGON ION SOURCE

J. S. Sovey
National Aeronautics and Space Administration
Lewis Research Center
Cleveland, Ohio 44135

Abstract

A 30-cm diameter argon ion source was evaluated. Ion source beam currents up to 4A were extracted with ion energies ranging from 0.2 to 1.5 KeV. An ion optics scaling relation was developed for predicting ion beam extraction capability as a function of total extraction voltage, gas type and screen grid open area. Ignition and emission characteristics of several hollow cathode geometries were assessed for purposes of defining discharge chamber and neutralizer cathodes. Also presented are ion beam profile characteristics which exhibit broad beam capability well suited for ion beam sputtering applications.

E-8917

Introduction

Recent studies of electric propulsion systems for orbit raising and on orbit operation of large space systems show potential advantages for employing large diameter ion thrusters using argon propellant.(1) Optimum design requirements imply thruster beam and discharge chamber currents a few factors higher than used in conventional mercury ion thrusters.(2) Argon ion sources are also used for ion milling, surface texturing and sputter deposition functions.(3,4) The development of broad beam capability is important for production processes involving ion beam milling or sputter deposition.

Argon ion thrusters and ion beam sputtering devices place different demands on component lifetime and source efficiency. The ion thruster system will require gas and power efficiencies in excess of 80 percent along with component lifetimes of at least 10,000 hours. Ion beam sputtering device applications allow component lifetimes and order of magnitude lower with easily replaceable components. Power and gas efficiency are important only as they effect capital equipment (such as power supplies and vacuum pumps) and piece part production costs.

The purpose of this investigation is to develop a broad ion beam sputtering device and evaluate potential components for large diameter argon ion thrusters. A 30-cm diameter ion beam sputtering device was tested using the most promising hollow cathodes and ion optics. Documentation of the ion beam profiles and current density range is presented.

Apparatus and Procedure

A section view of the 30-cm diameter ion source is shown in figure 1. Major elements of the ion source are the discharge chamber, ion optics (screen and accelerator grid), cathode and neutralizer. Ion source tests focused primarily on ion beam extraction capability, cathode emission characteristics and beam neutralization.

Ion Source Discharge Chambers

Four discharge chambers, described by Table I, were used in this study. The discharge chambers varied in the design of the magnetic circuit and the anode configurations. The basic magnetic circuit for discharge chambers A, B, and D was optimized by Bechtel(5) for a mercury ion thruster. Discharge chamber C contained the same pole pieces as the other configurations except the chamber length was extended to 20.5 cm in an attempt to improve ion source gas efficiency. Electromagnets were employed in all cases with the exception of discharge chamber A which used 14 permanent magnets. A three turn magnetic baffle coil which was capable of varying discharge chamber impedance was also tested. A 7.5 cm long mild steel collar (fig. 1) was employed on all ion sources. The collar shaped the magnetic field lines such that they intercept the anode, thereby providing lower discharge voltage operation. A 5-cm diameter mile steel baffle was used in all cases. All discharge chambers had cylindrical anodes whose length was 12 cm. Discharge chambers B and C also employed a rear anode which was mounted approximately in the plane of the baffle.

An 8-cm diameter ion source with a divergent magnetic field and hollow cathode discharge was used only to obtain ion optics scaling data. An ion source of this type is described in reference 6.

Ion Optics

The ion optics used in this study are described in Table II. All ion optics' grid plates were photochemically etched from arc cast molybdenum. The 30-cm diameter ion optics were dished away from the discharge chamber with a dish depth of 23 mm. The grid plates were spaced at the edge using synthetic mica and the grid to grid spacing at the periphery was 0.6±0.08 mm. The screen grid hole pattern of ion optics 3 was sized down (compensated) by 0.2 to 0.3 percent relative to the accelerator grid hole array. The compensation of the dished ion optics will yield a more paraxial beam as discussed in reference 7. Screen and accelerator grid hole patterns were matching (uncompensated) for all other sets of ion optics. All thirty centimeter diameter ion optics tests were conducted with discharge chamber C (Table I). Beam currents up to 4 A were extracted.

The 8 cm diameter ion optics (ion optics 5) were dished towards the discharge chamber with a dish depth of 2.5 mm.

Discharge Chamber Cathodes

Discharge chamber cathodes were fabricated from 6.4 mm diameter tantalum tubes. A 1.3 mm thick thoriated tungsten tip and a 1.7 cm diameter radiation flange were electron beam welded to the end of the tube. A porous tungsten cylindrical insert (0.56 cm o.d. x 0.28 cm i.d. x 2.5 cm long) impregnated with barium aluminate served as a dispenser of low work function material. The insert was positioned against the cathode tip. The only geometrical parameter varied was the cathode top orifice diameter. Orifice diameters employed were 0.76, 1.02, 1.52, 3.05 mm. The smallest orifice

cathode had a 90° chamfer with a 0.5 mm long throat. All other cathodes had straight through orifices.

Discharge chamber cathodes were started by applying a 3 kV, 3 μsec pulse to a probe located 2 mm from the face of the cathode tip.[8] Starting conditions are summarized in Table III.

Neutralizer Assemblies

Three neutralizer geometries were evaluated. Neutralizer A (fig. 2) was comprised of a tantalum tube, heater, cathode insert impregnated with barium aluminate, cathode tip with a 0.38 mm diameter orifice and a keeper electrode. Neutralizer B was identical to configuration A except the cathode tip was removed. Neutralizer C simply consisted of tantalum tube, heater and cathode insert.

Ignition of neutralizers A and B was accomplished after application of argon flow, 45 watts heater power and 400 volts to the keeper electrode. After neutralizer ignition, the keeper current was set at approximately 2 A, yielding keeper electrode voltages from 9 to 15 V. Total neutralizer emission, which is the sum of keeper and beam currents, ranged from 2 to 7 A.

Neutralizer C established a discharge directly to the beam plasma after the application of 90 watts heater power and approximately 3 equivalent amperes argon flow. Prior to ignition, neutralizer potential floated a few hundred volts negative with respect to ground.

Neutralizer A was positioned 9 cm radially from the last row of accelerator grid holes. Axial position was approximately 9 cm downstream of the screen pole piece. Figure 1 graphically defines neutralizer position. Neutralizers B and C were located approximately in the plane of the screen pole piece. The radial station was 9 cm from the last row of accelerator grid holes.

Neutralizer A was used during the ion optics and cathode investigations. Configurations B and C were employed during ion source beam diagnostic tests.

Facilities, Power Supplies and Feed System

Most ion source tests were conducted in a vacuum facility which was 3 m in diameter by 5.8 m long. Ion source beam diagnostics were performed in a vacuum chamber 1.5 m in diameter by 4.5 m long. The pumping capability of these facilities is shown in figure 3. Extremely high pumping speeds are required to adequately document performance of large diameter argon ion thrusters. For example, the 3 m diameter by 5.8 m long vacuum facility (fig. 3) consists of six high speed diffusion pumps each with a pumping capacity of 50,000 liter per second at an operating pressure of 10^{-6} torr. Deleterious effects due to high pressure operation (>10^{-5} torr) with the ion source include anomalously high accelerator grid currents due to charge exchange and discharge chamber gas ingestion from the facility. Facility requirements for ion beam sputtering devices are modest by comparison. Vacuum chamber pressures as high as 10^{-3} torr may be tolerated.[4]

Power to the ion source was provided by the seven supplies shown in figure 4. Steady state operation of the ion source involves operation of five power supplies as shown in the figure.

The gas feed system provides open loop control of the gas flow to the discharge chamber cathode, the ion source chamber and neutralizer. Argon flow rates were metered by hot tube anemometer flowmeters which were independently calibrated by a volume displacement meter. Approximately one equivalent ampere of argon flowed through the discharge chamber cathode during steady state operation. Total argon flow rates generally did not exceed eight equivalent amperes.

Feed system high voltage isolation was provided by synthetic rubber tubing whose length ranged from 50 to 100 cm.

Results and Discussion

Gas and power efficiency along with component lifetime play an extremely important role in the design of ion thrusters. Optimization of mercury ion thrusters indicate that the design of the magnetic circuit and ion optics have first order effects on power and gas efficiency.[9,10] The ion source magnetic circuit was optimized by Bechtel[5] for mercury operation. Electromagnets were used herein since higher magnetic field strengths were required for efficient operation as beam current levels were increased. The assessment of the effects of ion optics was a basic part of this investigation. The selection of discharge chamber cathode designs was based on the endurance test results of mercury hollow cathodes.[10] These studies indicate that increases in cathode orifice diameter and/or cathode tube diameter are required with increases in discharge current. The geometrical changes tend to limit the amount of local sputtering and self heating along with providing a lower temperature environment for the dispenser of low work function material. Low discharge chamber voltages (35 to 50 V) are desirable not only to limit cathode self heating but also to inhibit discharge chamber sputtering.

Efficiency and lifetime are less important as far as ion beam sputtering devices are concerned. Proper component selection and performance optimization, however, will yield long life ion sources, relatively simple power sources and possibly lower outlay for capital equipment. The argon ion source operation is assessed by evaluating major components (ion optics, cathode and neutralizer) for beam currents up to 4 A.

Tests were undertaken initially to evaluate the ion extraction capability of 30 cm and 8 cm ion sources using argon and xenon with various grid geometries. Next, the effects of ion optics on discharge chamber performance were assessed using the 30 cm diameter argon ion source with a fixed discharge chamber design. Further tests were performed to optimize the design of the discharge chamber cathode and neutralizer assemblies. Ion beam characteristics were obtained from an ion source specifically assembled for ion beam sputtering applications.

Ion Optics

Ion optics tests were performed using the 30 cm diameter ion source with discharge chamber C.

No attempt was made to optimize the discharge chamber for each set of ion optics. Tests were also undertaken with the 8 cm diameter ion source to develop an ion optics scaling relation.

Ion Beam Extraction Limits - Several sets of ion optics were evaluated to determine their beam current extraction capability. Childs law for parallel plates may be used to relate the space charge limited current to the minimum total extraction voltage for singly ionized species:

$$J_B = \text{constant} \cdot \frac{\Delta V^{3/2} A}{\sqrt{m}\, d^2}$$

where A is taken to be the screen grid open area (cm^2); m is the gas atomic weight (amu); J_B is the beam current (A); ΔV is the minimum total extraction voltage (V) and d is the effective ion accelerating distance. The total extraction voltage is the sum of the absolute magnitudes of the screen and accelerator grid voltages. The ion accelerating distance (which was not accurately known) is treated as a constant in the ion optics comparison. The value of the grid to grid spacing as measured at the periphery was 0.06±0.005 cm for all tests.

Figure 5 shows the variation of the beam current parameter, $J_B \frac{\sqrt{m}}{A}$, with minimum total extraction voltage. The minimum total extraction voltage, for each beam current parameter, is determined by the knee in the curve when ΔV is plotted against the accelerator grid current.(10) The figure displays data from three different sets of ion optics along with data from the 8 cm ion source. Gases include argon, xenon and mercury. The mercury ion optics performance was taken from reference 9. The data fall in a relatively narrow band allowing interpolation for predicting ion source beam extraction limits. Scatter in the data arises primarily from the variation of the effective ion accelerating distance and the differences in the ion density profile upstream of the screen grid.

Note that the beam current parameter increases with ΔV more rapidly than that predicted by Child's law. Effects that may produce deviations from Child's law such as variation of ion accelerating distance with beam current, multiply charged ions, and ions with initial velocities are alluded to in reference 11. The beam current parameter may be related to the total extraction voltage by the following relation:

$$\frac{J_B \sqrt{m}}{A} \approx 5.7 \times 10^{-9}\ \Delta V^{2.25} \pm 30 \text{ percent}$$

where the peripheral grid spacing is 0.06±0.008 cm. This scaling relation may be used to extrapolate ion source maximum beam current with total extraction voltage, gas type and screen grid open area as parameters.

Effect on Discharge Chamber Performance - Four sets of ion optics (Table II) were tested on ion source C to determine the effects of grid geometry on discharge chamber performance. Figure 6 shows the variation of discharge chamber losses (discharge energy per beam ion) with gas efficiency. The performance of ion optics 1 is poor due to low screen grid open area and a thick screen grid (0.51 mm). Ion optics 4 employs a thinner screen grid (0.38 mm) but the screen grid open area fraction was also low only 0.52. Ion optics 2 and 3 demonstrate the gains in performance due to higher screen grid open area. Highest performance was obtained with ion optics 3 which had the lowest accelerator grid open area fraction, 0.34. These results are similar to trends found in mercury ion thrusters.(9) The values of base level discharge chamber losses (190 eV/ion) are also comparable to results obtained from well optimized mercury ion thrusters.

In all tests flow rates were less than seven equivalent amperes of argon such that the effects of vacuum chamber gas ingestion would be less than one percent of the total flowrate. Gains in gas efficiency might be accomplished by refinements in discharge chamber magnetic circuit along with operation at higher magnetic field strengths. In this investigation the magnetic field strength was less than optimum for beam currents in excess of 3 A due to power supply and thermal limitations of the magnet wire insulation.

The effect of a decrease in accelerator grid open area on the discharge chamber V-I characteristic is shown in figure 7. A decrease in accelerator grid open area fraction from 0.49 to 0.34 results in approximately a 6 V decrease in discharge voltage over a rather wide range of discharge current.

Inspection of ion optics 3 revealed evidence of erosion near the centerline on the upstream surface of the accelerator grid. This suggests that for the discharge chamber geometry and screen grid geometries used, the accelerator grid hole diameter is near the minimum for beam currents exceeding 4A.

Discharge Chamber Cathode Performance

Cathode Starting - Cathodes were started by the application of 2 to 3 kV pulse to a molybdenum probe located 2 mm from the cathode tip. After the breakdown the discharge coupled directly to the anode. A cathode heater was not required. Table III lists the starting conditions for cathodes with orifice diameters of 0.76, 1.52, and 3.05 mm. Cathode starting was accomplished at lower flow rates with the small orifice designs. Cathodes were tested for periods only up to 200 hours, thus a long term assessment of cathode starting capability was not made.

Cathode Characteristics - A 30 cm diameter argon ion beam sputtering device requires discharge currents in the range 10 to 15 A. It is anticipated that argon ion thruster discharge current requirements will be considerably higher than 15 A. Because of power supply and facility limitations, cathode emission characteristics were documented only over a 10 to 25 A range.

The cathode geometries were nearly identical

to those used on 30 cm diameter mercury ion thrusters.[2] The only variable was cathode orifice diameter. As mentioned earlier, a significant amount of data exist concerning hollow cathode lifetime assessment. Cathode erosion rates may be adequately correlated with discharge current level and cathode orifice diameter.[10,12] It was desired to obtain a cathode that exhibited the following: ease of starting, low thermal loading due to discharge self heating, stability during a high voltage recycle and an acceptable V-I characteristic for discharge currents from 10 to 25 A.

Figure 8 illustrates the variation of discharge voltage with discharge chamber magnetic field strength for cathodes with orifice diameters of 0.76 and 1.52 mm. The smaller orifice cathode generally exhibited high discharge voltage for currents from 10 to 20 A at magnetic field strengths necessary to obtain discharge chamber losses less than 250 eV/ion.

Figure 9 shows the V-I characteristics of discharge chamber D employing cathodes with orifice diameters of 0.76 and 1.02 mm. The smaller orifice cathode yields lower beam current and higher discharge voltage operation for a fixed discharge current. High discharge voltage operation at low discharge currents does not lend itself well to high voltage recycle techniques which involve cutback of the discharge current. In this type of recycle, the discharge became unstable and sometimes extinguished. High voltage recycle sequences that reduce the electromagnet current, however, are effective.

The cathode with the 0.76 mm diameter orifice showed evidence of relatively high discharge self heating and sputter erosion. Such evidence includes visual observation of high cathode brightness and also thermal distortion of the 0.25 mm cathode tube wall. Enlargement of the cathode orifice by approximately 0.13 mm over a period of 200 hours was observed.

Larger orifice cathodes were investigated using discharge chambers A and B. Figure 10 shows the discharge V-I characteristics of cathodes with 1.52 and 3.05 mm diameter orifices. Discharge chamber A characteristics indicate that by using the larger orifice cathode there is approximately a 5 V reduction in discharge voltage at 20 A discharge current and lower discharge chamber losses. Note, however, that further reductions in discharge voltage may be obtained by employing a rear anode (discharge chamber B). The long collar (fig. 1) tends to shunt the magnetic circuit and apparently provide a large electron interaction region and allow electrons easy access to the anodes. The cathode with the 1.52 mm diameter orifice demonstrated best overall performance for the discharge chambers used in this investigation. No measurable cathode orifice erosion (<0.02 mm) was detected after 150 hours of operation.

Neutralizer Performance

A neutralizer is required for all ion thruster applications to avoid beam or spacecraft charge build-up. For some ion beam sputtering applications the neutralizer may be deleted if ion energies exceed 1000 eV and there exists an adequate ground return circuit. For ion energies less than 500 eV an active neutralizer was required to prevent cycling of screen and accelerator grid voltages.

Neutralizer cathode A (fig. 2) is similar in geometry to those employed in mercury ion thrusters where 4 A total emission is required.[2] The argon neutralizer differs, however, since an enclosed keeper electrode configuration is necessary to provide high gas pressure for ease of ignition.

The procedure for igniting and establishing a plasma bridge to the ion beam for three different neutralizer assemblies has been described earlier. Beam neutralization ability of each configuration was also addressed. A measure of the neutralization capability is the system floating voltage and flow rate requirements. System floating voltage is the potential difference between neutralizer and ground (fig. 4).

Beam neutralization capability of configurations A, B, and C is shown in figure 11. For beam currents between 2 and 2.5 A the floating voltage could be maintained below 30 V with less than 1.0 equivalent amperes argon flow rate. With the application of cathode heater power, lower levels of floating voltage are attained. Enhanced electron emission occurred with the application of cathode heater power for all neutralizer configurations. This effect, which is important at low emission currents, is best shown by neutralizer C whose total emission current is 2A versus 4 A for neutralizers A and B.

Neutralizers B and C yield operation at lower levels of floating voltage. However, the data for neutralizers B and C were taken at 2 versus 2.5 A beam current for neutralizer A. As beam current levels increase, the neutralizer cathode self heating increases, the heater plays a lesser role and higher argon flow rates are required to maintain a given floating voltage.

Neutralizer C which is simply composed of a tantalum tube, insert and heater operates effectively at flow rates as low as 200 equivalent mA of argon. The plasma bridge reestablishes after high voltage recycle without the aid of additional heater power.

Since each neutralizer assembly was tested for periods of 200 hours or less, a lifetime assessment was not made. Neutralizer A, however, showed evidence of embrittlement of the tantalum tube. This was possibly due to a tantalum-alumina reaction at high temperature. Neutralizers A and B also showed some distortion of the keeper electrode orifice after long term operation.

For ion beam sputtering devices, neutralizer C appears to be the best candidate because of design simplicity and ease of replacement.

Ion Source Beam Characteristics

One of the major objectives of this study was to develop a broad beam ion source for ion machining and sputter deposition applications. An ion source was assembled using discharge chamber D, ion optics 3, a discharge chamber cathode with a 1.52 mm diameter orifice and neutralizer B. Ion beam surveys were made with a negatively biased planar probe. Distance from the ion optics to the beam

probe was 15 cm.

Figure 12 shows the variation of beam current density (center of the ion source) for various beam currents and beam energies. The ion source current density ranged from 0.4 to 3 mA/cm^2 at beam energies from 200 to 1500 eV. The ion source operating envelop was limited by the screen power supply whose maximum output was 2.2 kW.

Figure 13 shows radial surveys at low and high beam current density at beam energies of 200 to 500 eV, respectively. At low current densities the beam exhibits a relatively flat profile over a 25 cm diameter. The profile becomes bell shaped at higher current densities.

The effect of beam energy on the shape of the beam profile is shown in figure 14. At higher energies the beam profile exhibits higher centerline current densities. This effect is probably due to the variation in the ratio of net to total accelerating voltage, redistribution of ion current density upstream of the screen grid or enhancement of secondary electron emission at the probe. At a beam energy of 500 V the beam current density varies by approximately ±13 percent over a region 25 cm in diameter. Further gains in ion beam uniformity might be made by magnetic circuit optimization along with ion optics corrective grid misalinement.(7,10)

Conclusions

Ion optics, cathodes and neutralizers for a 30 cm diameter argon ion source were evaluated. Significant test results are as follows:

1. An ion optics scaling relation was developed for predicting ion source beam extraction capability. The ion optics parametric data was generated using 30 cm and 8 cm diameter ion sources with argon and xenon gases. Mercury ion source data was also included. The scaling relation may be used to extrapolate ion source maximum beam current with total extraction voltage, gas type and screen grid open area as parameters.
2. Using ion optics with screen and accelerator grid open area fractions of 0.67 and 0.34, respectively, resulted in highest discharge chamber performance. Minimum discharge chamber losses were 190 eV/ion with maximum gas efficiency in excess of 0.70.
3. A 6.4 mm diameter cathode with a 1.52 mm diameter orifice exhibited the best overall performance which included ease of starting, low discharge voltage operation and extended lifetime for discharge chamber currents from 10 to 25 A.
4. A neutralizer consisting of a 6.4 mm diameter tantalum tube, a porous tungsten barriated insert and a heater operated effectively at a beam current of 2 A with an argon flow rate as low as 200 equivalent mA.

An ion source was assembled and tested for purposes of ion beam sputtering applications. The ion source current density ranged from 0.4 to 3 mA/cm^2 at beam energies from 200 to 1500 eV. At a beam energy of 500 eV, the beam uniformity was ±13 percent over a region 25 cm in diameter at a distance 15 cm downstream of the ion optics.

References

1. Byers, D. C., Rawlin, V. K., "Electron-Bombardment Propulsion System Characteristics for Large Space Systems," Paper No. 76-1039, to be presented at AIAA 12th Electric Propulsion Conference, Key Biscayne, Fla., Nov. 1976.

2. Schnelker, D. E., Collett, C. R., "30-Cm Engineering Model Thruster Design and Qualification Tests," Paper No. 75-341, AIAA 11th Electric Propulsion Conference, New Orleans, La., Mar. 1975.

3. Spencer, E. G. and Schmidt, P. H., "Ion Beam Techniques for Device Fabrication," Journal of Vacuum Science and Technology, Vol. 8, Sept.-Oct. 1971, pp. S52-S70.

4. Reader, P. D. and Kaufman, H. R., "Optimization of an Electron-Bombardment Ion Source for Ion Machining Applications," Journal of Vacuum Science and Technology, Vol. 12, Nov.-Dec. 1975, pp. 1344-1347.

5. Bechtel, R. T., "Performance and Control of a 30-Cm-Diam, Low Impulse, Kaufman Thruster," Journal of Spacecraft and Rockets, Vol. 7, Jan. 1970, pp. 21-25.

6. Hudson, W. R., "Nonpropulsive Applications of Ion Beams," Paper No. 76-1015, to be presented at 12th Electric Propulsion Conference, Nov. 1976, Key Biscayne, Fla., Nov. 1976.

7. Danilowicz, R. C., et al, "Measurement of Beam Divergence of 30-Cm-Diameter Dished Grids," Paper No. 73-1051, AIAA 10th Electric Propulsion Conference, Lake Tahoe, Nev., Oct.-Nov. 1973.

8. Wintucky, E. G., "High Voltage Pulse Ignition of Mercury Discharge Hollow Cathodes," Paper No. 73-1140, AIAA 10th Electric Propulsion Conference, Lake Tahoe, Nev., Oct.-Nov. 1973.

9. Rawlin, V. K., "Performance of 30-Cm-Ion Thrusters with Dished Accelerator Grids," Paper No. 73-1053, AIAA 10th Electric Propulsion Conference, Lake Tahoe, Nev., Oct.-Nov. 1973.

10. Kaufman, H. R., "Technology of Electron-Bombardment Ion Thrusters," Advances in Electronics and Electron Physics, vol. 36, Academic Press, New York, 1974, pp. 265-373.

11. Rawlin, V. K., "Studies of Dished Accelerator Grids for 30-Cm-Ion Thrusters," Paper No. 73-1086, AIAA 10th Electric Propulsion Conference, Lake Tahoe, Nev., Oct.-Nov. 1973.

12. Mirtich, M. J., "Investigation of Hollow Cathode Performance for 30-Cm Thrusters," Paper No. 73-1138, AIAA 10th Electric Propulsion Conference, Lake Tahoe, Nev., Oct.-Nov. 1973.

TABLE I. - DISCHARGE CHAMBER DESCRIPTION (BASIC DESIGN: REF. 5)

Ion source	Magnet type	Number of magnets	Magnet current, A	Range of Bz from baffle to plane of screen, pole piece, gauss	Distance from baffle to plane of screen pole piece, cm	Rear anode
A	PM	14	NA	20-4	10	No
B	EM	25	15	40-10	10	Yes
			10	29-7		
C	EM	26	15	34-2	18	Yes
			10	27-1		
D	EM	25	10	29-7	10	No

NA: Not apply.

TABLE II. - ION OPTICS GEOMETRY

Ion optics		Hole diam., mm		Grid thickness, mm		Open area fraction		Dish depth, mm
S/N	Dia., cm	Screen	Accelerator	Screen	Accelerator	Screen	Accelerator	
1	30	1.57	1.57	0.51	0.51	0.46	0.46	23
2	30	1.93	1.62	.38	.51	.69	.49	23
3	30	1.91	1.37	.38	.51	.67	.34	23
4	30	1.32	1.32	.38	.38	.52	.52	23
5	8	1.97	0.89-0.64	.38	.38	.725	----	2.5

TABLE III. - HOLLOW CATHODE STARTING CHARACTERISTICS FOR ARGON

Cathode type	Cathode orifice diam., mm	Cathode heater power, W	Starting voltage	Main flow, eq. A	Cathode flow, eq. A
Main cathode	0.76	0	2-3 kV pulse	5	1-4.5
Main cathode	1.52	0	2-3 kV pulse	5	5-15
Main cathode	3.05	0	2-3 kV pulse	5	10-15
Neutralizer A	.38	45	400 V	NA	1-5
Neutralizer B	2.8	45	400 V	NA	1-5
Neutralizer C	2.8	90	NA	NA	2.5-3.5

NA: Not apply.

E-8917

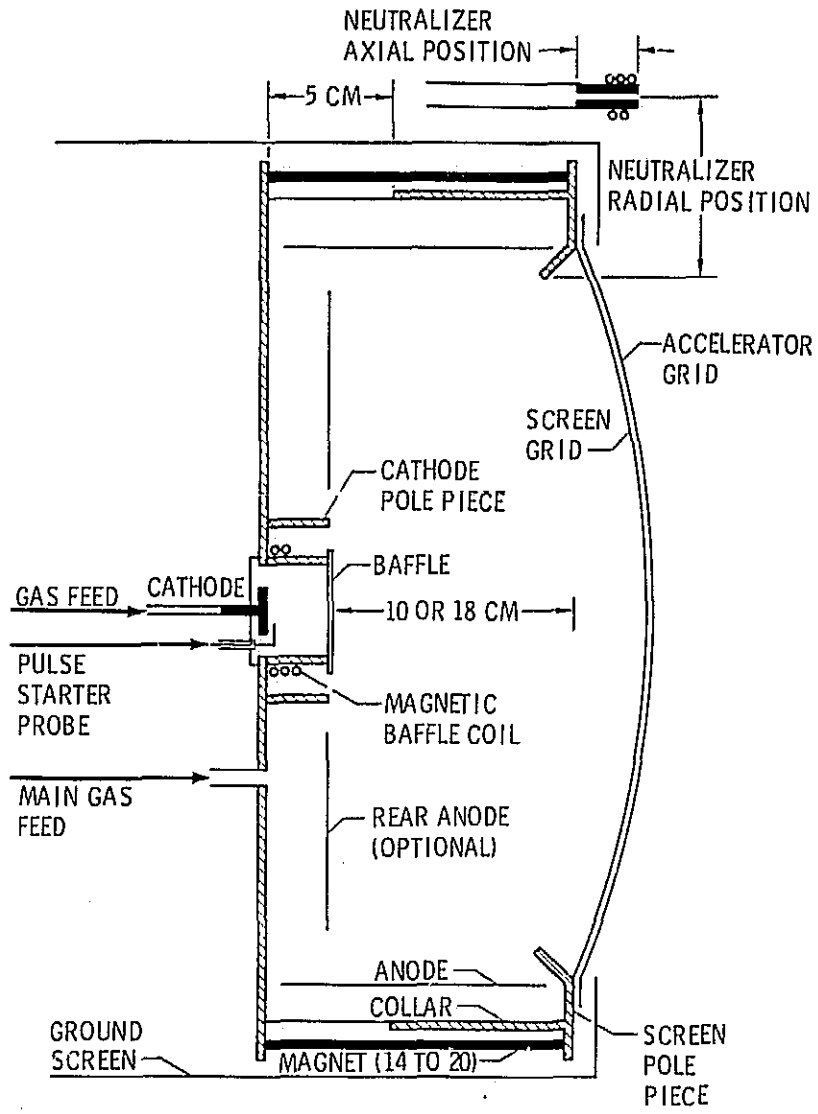

Figure 1. - Section view of 30 centimeter diameter ion source.

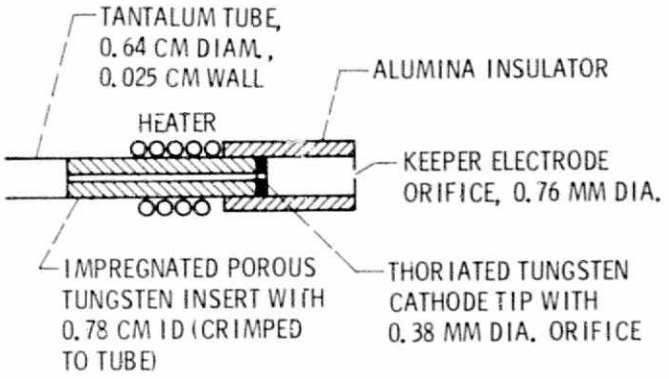

(a) NEUTRALIZER A.

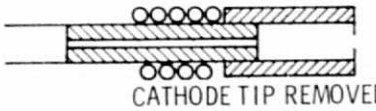

(b) NEUTRALIZER B.

(c) NEUTRALIZER C.

Figure 2. - Sketch of neutralizer assemblies.

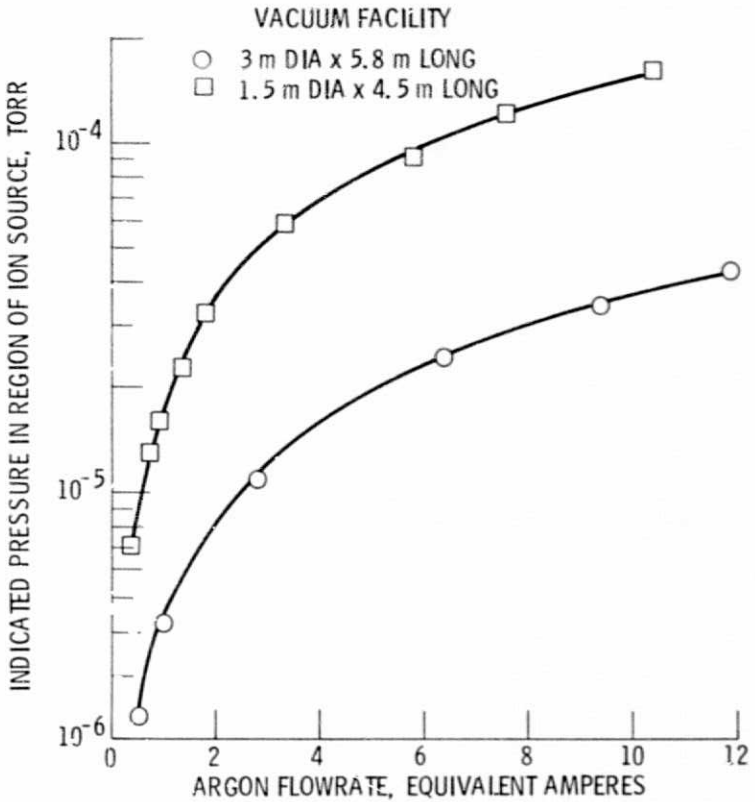

Figure 3. - Effect of argon gas loading on vacuum facility pressure.

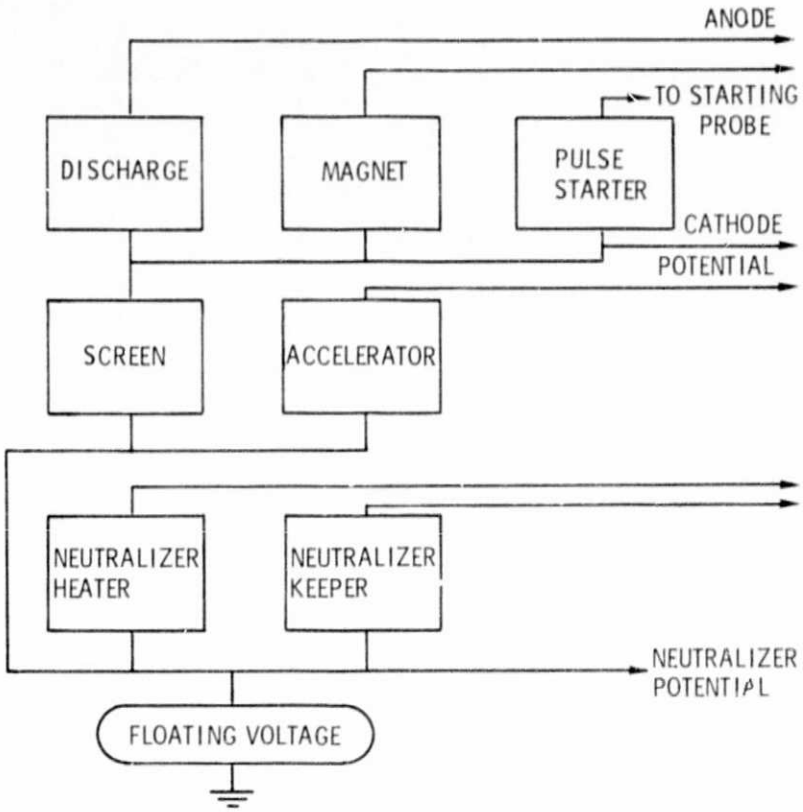

POWER SUPPLY REQUIREMENTS			
POWER SUPPLY	START-UP	RUN WITH NEUTRALIZERS A, B	RUN WITH NEUTRALIZER C
SCREEN		•	•
ACCELERATOR		•	•
DISCHARGE	•	•	•
PULSE STARTER	•		
NEUT. HEATER	•		•
NEUT. KEEPER	•	•	
MAGNET		•	•

Figure 4. - Schematic of power supplies.

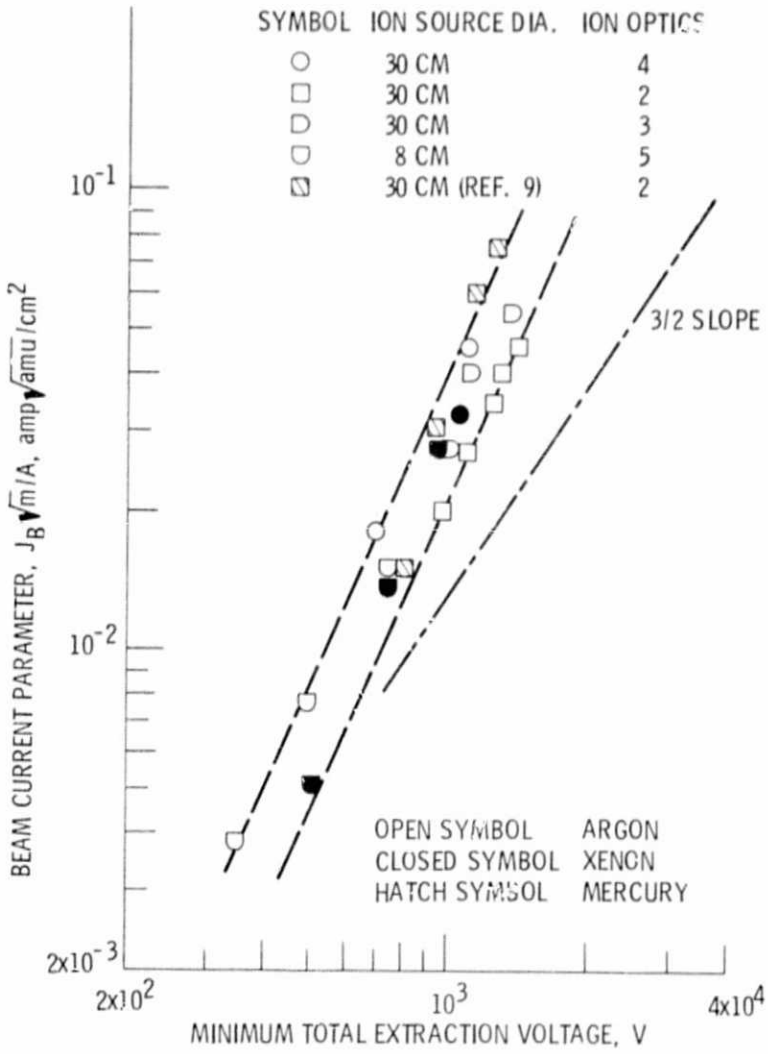

Figure 5. - Gas ion source ion optics characteristics. Grid to grid spacing at perimeter: ≈ 0.6 mm; A: screen grid open area, m: gas atomic weight.

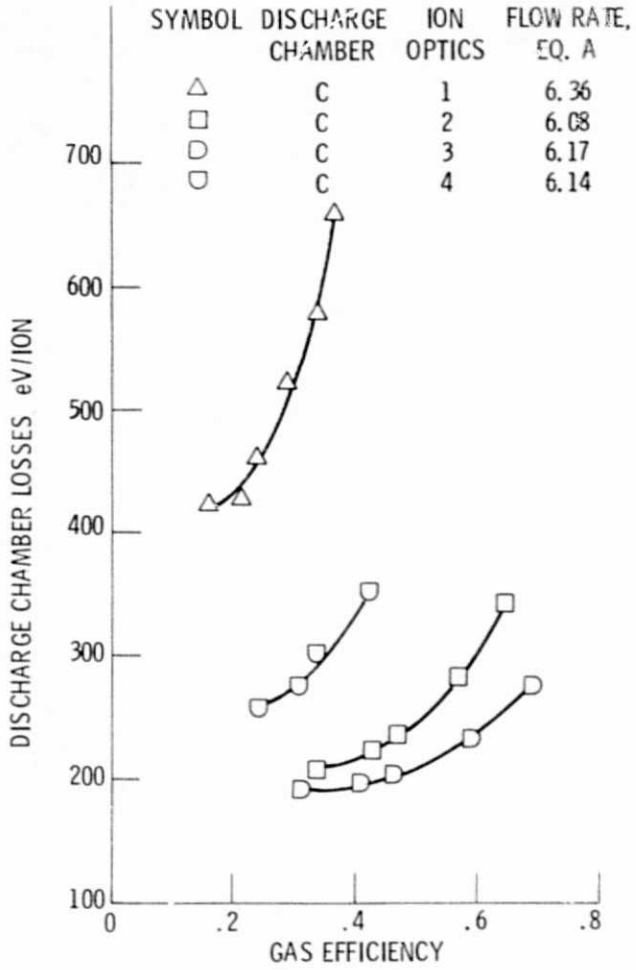

Figure 6. - Discharge chamber performance variation with ion optics geometry. Argon gas; magnet current, 15 A.

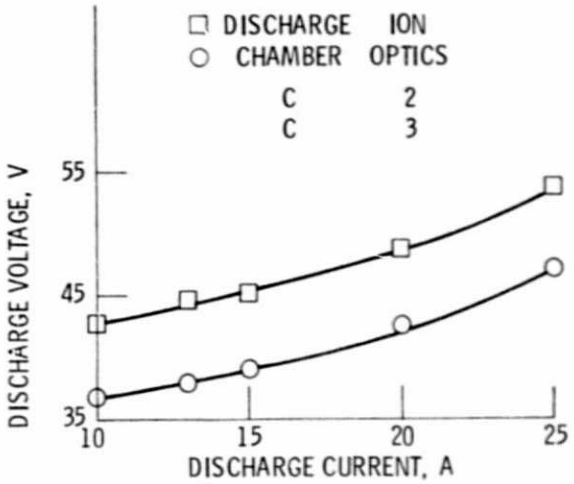

Figure 7. - Effect of accelerator grid open area on the discharge characteristic. Argon flow rate: 6.15 equivalent A.

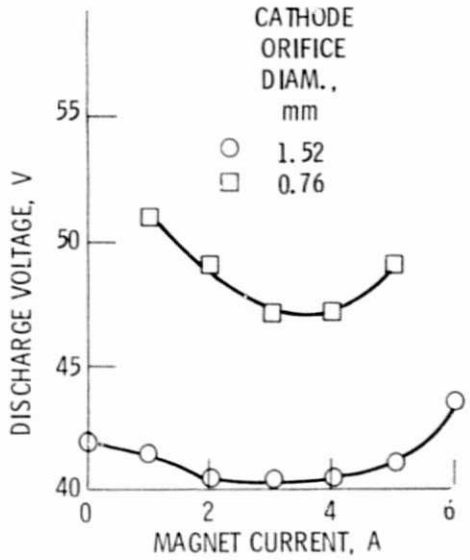

Figure 8. - Effect of magnetic field strength on discharge voltage for two cathode orifice diameters. Discharge chamber, D. Ion optics 2; discharge current, 10 A.

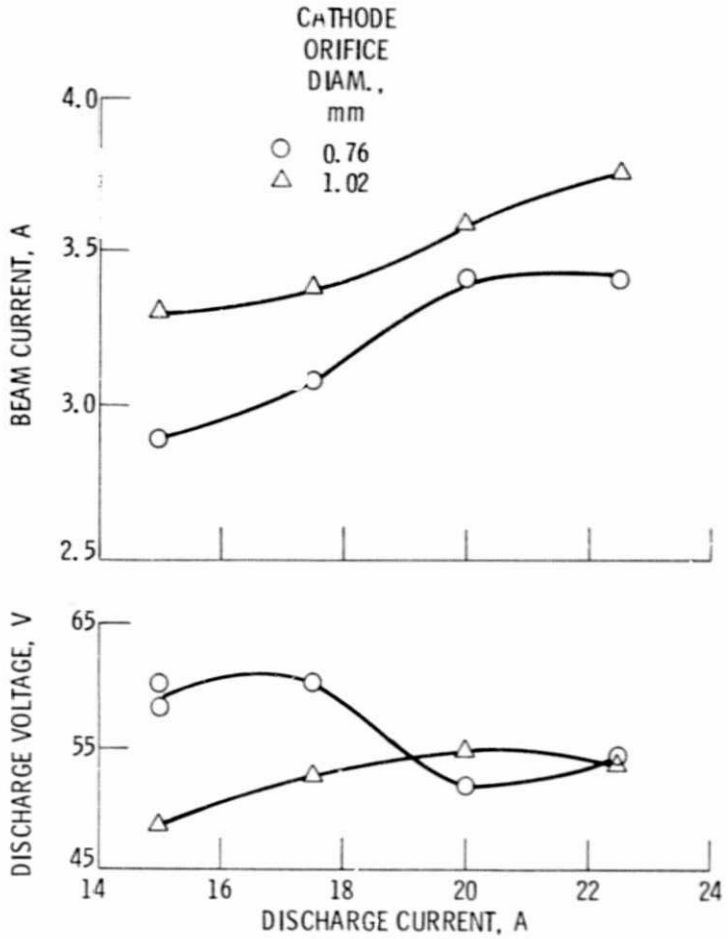

Figure 9. - Discharge chamber performance with small cathode orifice diameter. Magnet current = 10-11 A. Ion optics 2; argon flow rate: 6.1 equivalent A; discharge chamber D.

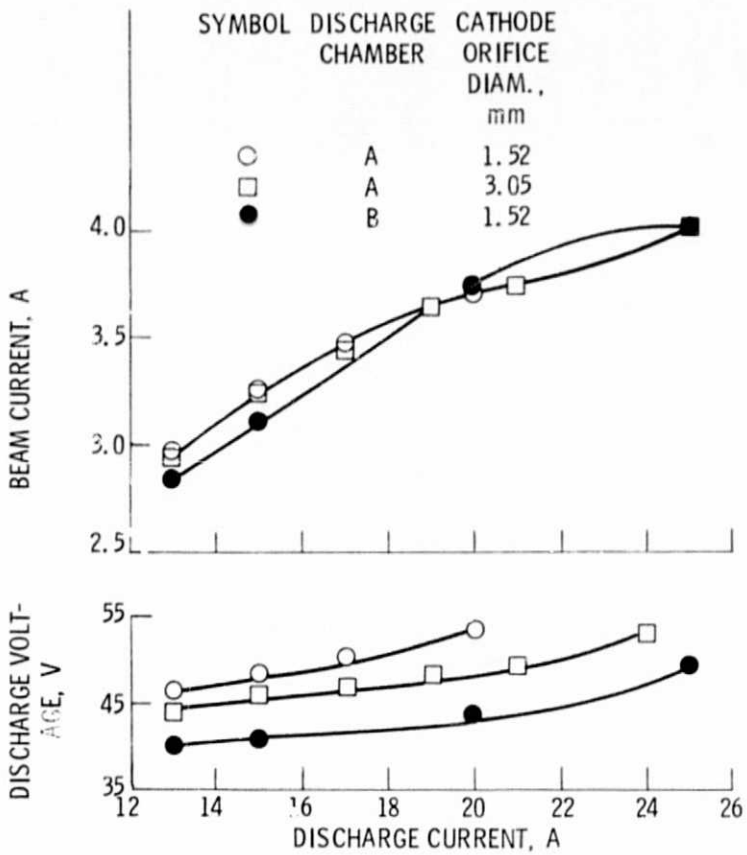

Figure 10. - Discharge chamber performance with large cathode orifice diameter. Ion optics 3; argon flowrate: 6.1 equivalent A.

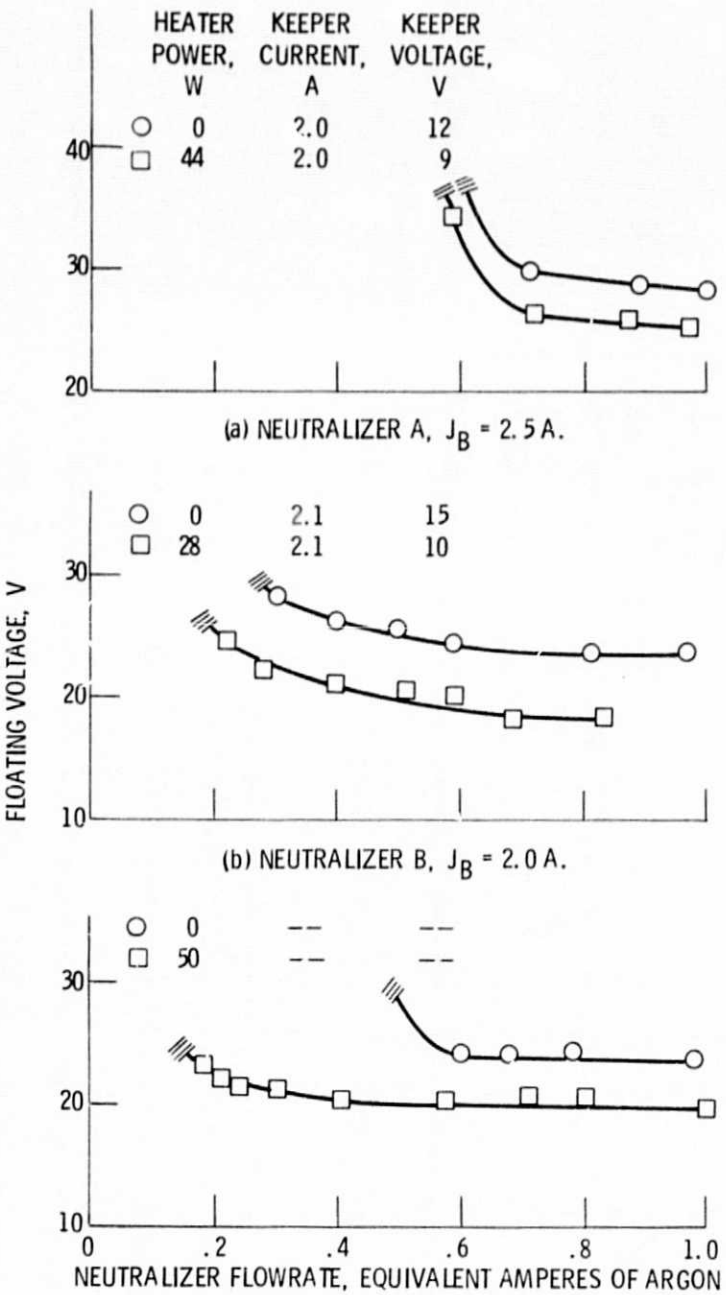

Figure 11. - Argon neutralizer characteristic for three cathode configurations; beam energy, 1000 eV.

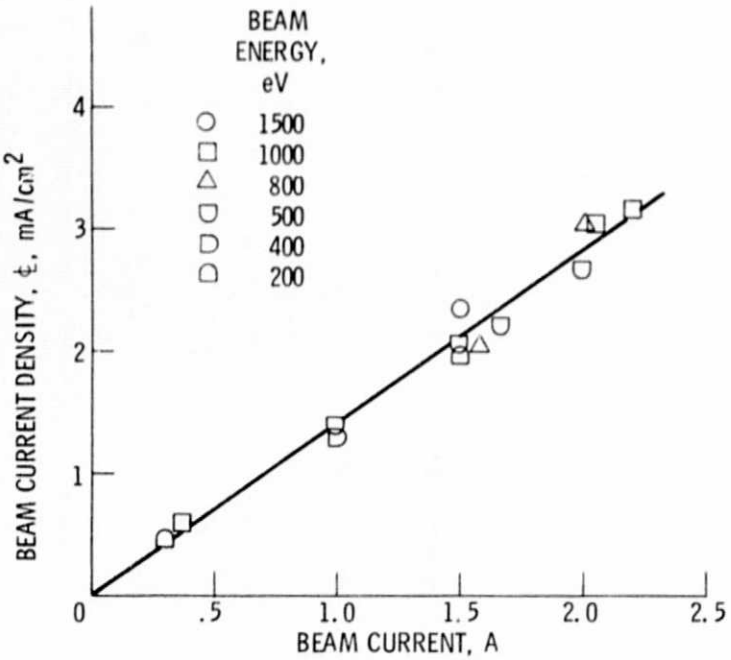

Figure 12. - Variation of centerline beam current density at various beam current and beam energies. Distance from beam probe to ion optics: 15 cm.

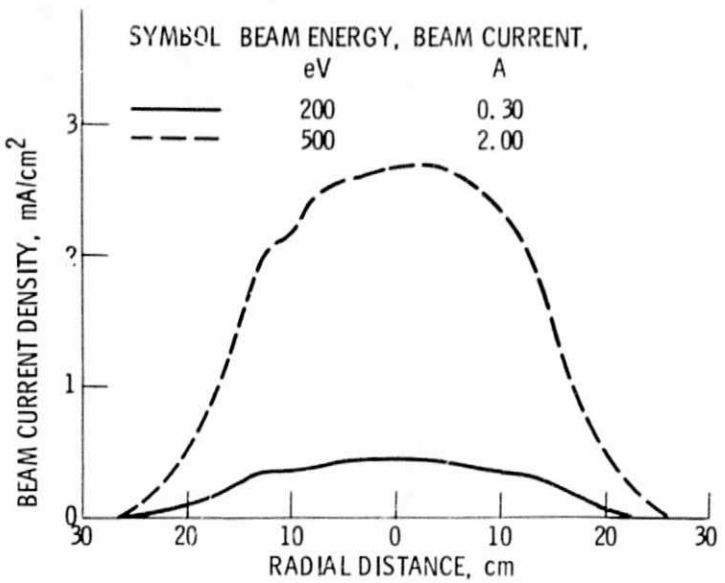

Figure 13. - Argon ion source beam profiles at different beam power levels. Beam probe-ion optics separation: 15 cm, ratio of net to total extraction voltage, 0.5.

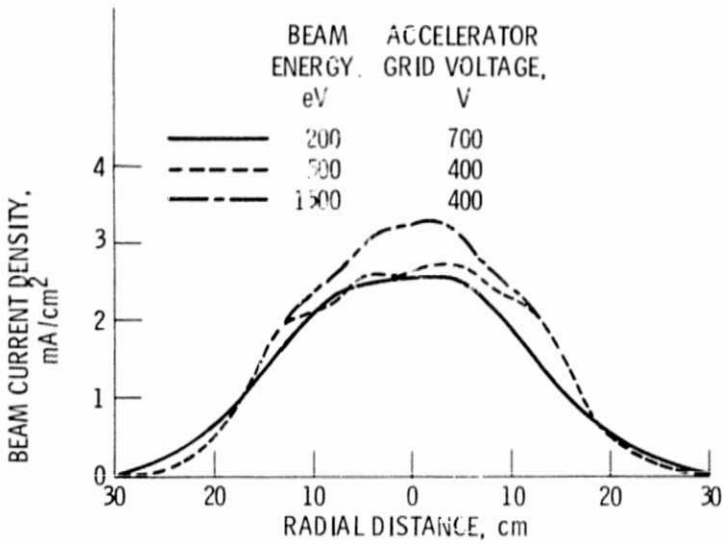

Figure 14. - Argon ion source beam profiles for various beam energies. Beam probe-ion optics separation: 15 cm, beam current, 1.5-1.6 A.